Indian J Phys (September 2024) 98(10):3535–3543
https://doi.org/10.1007/s12648-024-03139-x

ORIGINAL PAPER

Numerical study of high emissivity metamaterials for radiative cooling application

W Minalu[1] and F Tolessa[2]*

[1]Department of Physics, College of Natural and Computational Science, Mizan-Tepi University, Tepi, Ethiopia

[2]Department of Applied Physics, School of Applied Natural Science, Adama Science and Technology University, Adama, Ethiopia

Received: 10 July 2023 / Accepted: 15 February 2024 / Published online: 18 March 2024

Abstract: In this research, we designed a disc structure metamaterial emitter using silver and titanium dioxide for radiative cooling applications. We used COMSOL Multiphysics software for numerical simulations, considering temperature changes induced by atmospheric and surface radiation. The results of the numerical simulations demonstrated that the designed emitter had an average emissivity of 89.5% within the atmospheric transparency window, which spans from 8 to 13 µm. Furthermore, the designed emitter has the potential to achieve a radiative cooling power of 200.4 W/m^2 at an ambient temperature of 300 K and can reach an equilibrium temperature of 268.25 K. Impressively, the designed emitter can cool down to 31.75 °C below the ambient temperature. Based on the results of our research, metamaterial emitter has the potential to be crucial components in the development of energy-efficient radiative cooling devices. Therefore, this work further contributes to the advancement of passive radiative coolers based on metal–dielectric–metal.

Keywords: Radiative cooling; Metamaterials; High emissivity; Atmospheric window

1. Introduction

Metamaterials electromagnetic properties are described based on the effective parameters, and these materials usually gain their properties from structure rather than composition [1]. They have demonstrated the ability to achieve exotic properties which is difficult to attain naturally on materials. One of the extraordinary properties explored on metamaterials (MM) is negative refractive index predicted theoretically in 1968 and experimentally demonstrated in 2000. Since then, the research into MM has grown enormously resulting in many novel phenomena including invisibility, cloaks, and perfect lenses [2]. One of the interesting uses of MM has been the development of the so-called ''perfect absorber'', which exhibits the ability to yield near-unity (100%) absorptivity in nearly all frequency ranges.

According to Kirchhoff's law of thermal radiation, at the equilibrium, the emissivity of a material is equal to its absorptivity. Therefore, in principle MM perfect absorbers radiate energy described by their absorptivity, at a given temperature. Because of the resonant nature of MM the perfect absorber yields sharp resonances with high absorption, thus high heat emitters with high emissivity [3, 4].

A passive cooling technique cools without power input, therefore making a great difference in energy conservation and emissions reduction. Such strategies do not need to cover all of the cooling loads of a space, but should be able to ease the reliance on conventional systems. Passive radiative cooling (PRC) possesses enticing potential for reducing energy use in buildings and is one of the viable alternatives in this regard. It is a natural method of cooling buildings with least expensive, and it mainly depends on interaction of building and its surrounding [2, 5]. The universe can be utilized as a sink for heat pumping by means of passive radiative cooling [6].

The Earth's atmosphere is almost transparent to the emitted radiation from an object, between the wavelengths of 8 and 13 µm. This means that almost all radiative energy within this band can be easily lost to the sky and helps the objects cool off. The key to obtain radiative cooling is to create an imbalance between the absorbed radiation from the environment and the heat radiated outwards through the atmospheric window [7]. One of the key challenges is

*Corresponding author, E-mail: tolasaa21@astu.edu.et

designing an emitter that emits electromagnetic radiation in certain wavelength ranges. Overall, many efforts have been dedicated to design and optimize the high infrared emission within the required atmospheric window 8–13 μm wavelength regions. In this study, we have improved the performance of the emitter for radiative cooling application, with the aim to understand how to improve its associated problems of manufacturing and design for radiative cooling applications. But, the realization of such ideal emitters for effective radiative cooling has always been a challenge. The largest cooling power demand usually occurs at daytime under the direct sunlight, which is more challenging due to the incident solar irradiation. However, earlier works are limited to night-time cooling, because it is difficult to simultaneously realize high reflectivity in the solar spectrum and high emissivity in the atmospheric transparency window [8].

2. Fundamental principles of radiative cooling

To realize radiative cooling, two main concepts should be understood. First, from thermodynamics, it is known that heat will spontaneously flow from a hot to a cold body. Therefore, heat from high temperature terrestrial bodies ($\sim$ 300 K) can always flow towards a low-temperature sink, the biggest and lowest of all being outer space (3 K). Second, there is a transparent window in the atmosphere (8–13 μm) that can be used to exchange heat between the Earth and outer space in the form of infrared radiation. Radiative cooling exploits these concepts to achieve energy-free cooling. An ideal radiative cooling system would have 100% reflectance over the whole solar spectrum while simultaneously having 100% thermal emission in atmospheric window. By optimizing a MM design these two conditions can be satisfied, so passive energy-free cooling can be achieved [9].

As the radiator is exposed to a clear sky, it has subjected to the combined effects of its own infrared radiation, solar irradiance, atmospheric thermal radiation and non-radiation term. Assuming ambient temperature and radiator surface temperature are T_{amb} and T_{s}, respectively. The net cooling power is given by [10]:

$$P_{\mathrm{net}}(T_{\mathrm{s}}) = P_{\mathrm{rad}}(T_{\mathrm{s}}) - P_{\mathrm{atm}}(T_{\mathrm{amb}}) - P_{\mathrm{sun}} - P_{\mathrm{cond+conv.}} \quad (1)$$

In Eq. (1), the emissivity power by the structure or the radiative power emitted by MM cooler is given by [11]:

$$P_{\mathrm{rad}}(T_{\mathrm{s}}) = \int d\Omega \cos\theta \int_0^{\infty} I_{\mathrm{BB}}(T_{\mathrm{s}}, \lambda)\varepsilon(\lambda, \theta) d\lambda, \quad (2)$$

$$P_{\mathrm{atm}}(T_{\mathrm{amb}}) = \int d\Omega \cos\theta \int_0^{\infty} I_{\mathrm{BB}}(T_{\mathrm{amb}}, \lambda)\varepsilon(\lambda, \theta)\varepsilon_{atm}(\lambda, \theta) d\lambda \quad (3)$$

$$P_{\mathrm{sun}} = \int_0^{\infty} I_{\mathrm{AM1.5}}(\lambda)\varepsilon(\lambda, \theta) d\lambda \quad (4)$$

$$P_{\mathrm{cond+conv}} = h_{\mathrm{c}}(T_{\mathrm{atm}} - T_{\mathrm{s}}) \quad (5)$$

Here, $\int d\Omega = 2\pi \int_0^{\pi/2} \sin\theta d\theta$ is the angular integral over a hemisphere.

$\varepsilon(\lambda, \theta)$ is the angular spectral emissivity of the atmosphere, which can be calculated by:

$$\varepsilon_{\mathrm{atm}}(\lambda, \theta) = 1 - t(\lambda)^{1/\cos\theta}. \quad (6)$$

where $P_{\mathrm{rad}}(T_{\mathrm{s}})$ is emissivity power of radiator surface, $P_{\mathrm{atm}}(T_{\mathrm{amb}})$ is the absorbed power due to the incident atmospheric thermal radiation, P_{sun} is the absorbed sun power, $P_{\mathrm{cond+conv}}$ are the power absorbed by conduction and convection, T_{s} is the temperature of radiator, T_{amb} is ambient temperature of environment, λ corresponds to the wavelength of the incident electromagnetic wave, $\varepsilon(\lambda, \theta)$ is the spectral directional absorptivity of the radiator, and $t(\lambda)$ is the atmospheric transmission in the zenith direction.

All solid surfaces radiate heat in the form of electromagnetic radiation, whose power is proportional to temperature and emissivity, and is distributed across the frequency spectrum [3, 12]. Thus, the term total emissive power is differentiated from spectral emissive power, where the former refers to energy emitted over the entire spectrum, while the latter suggests energy emitted at a specific wavelength interval. The spectral emissive power of an ideal blackbody is governed by Planck's law as stated by [12].

$$I_{\mathrm{BB}}(T_{\mathrm{s}}, \lambda) = \frac{2hc_0^2}{\lambda^5[e^{hc_0/\lambda k_B T} - 1]} \quad (7)$$

where $I_{\mathrm{BB}}(T_{\mathrm{s}}, \lambda)$ is the spectral emissive power of a blackbody at a certain temperature T_{s} for a particular wavelength λ, h is the Planck's constant (6.626×10^{-34} J s), k_{B} is the Boltzmann constant (1.3807×10^{-23} J/K), and c_0 is speed of light in vacuum (2.998×10^{8} m/s) [11].

3. Materials and methods

3.1. Numerical analysis (COMSOL Multiphysics)

We have used COMSOL Multiphysics software to carry out this study. The MM emitter was designed from Silver (Ag) and Titanium dioxide (TiO_2) using COMSOL Multiphysics software. Three dimensions (*x*-axis, *y*-axis, and *z*-axis) are selected for working environment. The optics interface has been used in order to compute electric and magnetic fields for our system, where the wavelength is comparable to or much smaller than the studied device. Electromagnetic wave frequency domain interface is selected to solve for time harmonic electromagnetic field distributions. The wavelength domain study is used to compute the response of model subjected to harmonic excitation for one or several wavelengths. In electromagnetic wave propagation through the designed structure, it is used to compute a structure's transmission and reflection versus wavelength. For the designed disc structure, the following parameters such as width of unit cell (w), height of disc (h_1), thickness of dielectric (h_2), thickness of ground metal (h_3), and radius (r) of disc were considered. The designed MM consists metal–dielectric–metal.

Numerical simulation was conducted on the single unit cell with the intention of decrease computational time. A three-dimensional electromagnetic wave and the wavelength domain study were performed using COMSOL Multiphysics software. During the numerical analysis, perfectly matched layer was assigned on the top and bottom of the computational domains or along z-axis to minimize reflection. The periodic boundary condition was also set at both the right side and left side boundaries to account for an infinite flat surface on the emitter and also for oblique incidence. The electromagnetic waves or incident light on the emitter is considered to be perpendicular to the x–y plane through the working wavelength. The refractive index (optical properties) of Silver (Ag) and the dielectric spacer Titanium dioxide (TiO_2) were taken from the default material list of the software. Titanium dioxide (TiO_2) was considered because of its small absorptivity in the visible and near-infrared, but high absorptivity in the mid-infrared region (8–13 μm) spectrum. Besides, TiO_2 is a high-index material and it is transparent in the other wavelengths of thermal infrared. All these features make TiO_2 a favourable material for the radiative emitter. It is well known that a metal such as Ag has high reflection in the solar spectrum which fits this radiative cooling application well. Also, adding Ag layer increases the absorption in the 8–13 μm interval [13, 14].

4. Results and discussion

4.1. Result

The designed MM emitter has a three-layer structure as demonstrated in Fig. 1 underneath. The top layer is composed of a Silver (Ag) array with a periodicity of w. A unit cell has a layer, designed from Ag and TiO_2 with height (h_1) of disc and radius (r). A thin film of Titanium dioxide (TiO_2) has thickness (h_2) is designed on the top of a Silver (Ag) film of thickness (h_3), which acts as a perfect reflector.

The height (h_1) of disc is 0.95 μm, and the thickness (h_3) of the ground metal is 2 μm; these parameters were remaining fixed. In contrast, width (w) of the unit cell, radius (r) of the disc and thickness (h_2) of dielectric layer vary. Titanium dioxide (TiO_2) is introduced as the dielectric layer with thickness (h_2). Silver (Ag) introduced as substrate with a thickness (h_3) was selected to prevent transmission of the incident light. Electromagnetic wave of frequency 300 THz released from the in port to our designed emitter by COMSOL Multiphysics.

A lot of parameters such as height, width of unit cell, and radius of top metal are optimized, and the below result was obtained. In the next sub-topics, the effect of variable parameters on the emissivity and cooling power of our designed emitter was discussed. Finally, comparison between the emissivity of the designed MM emitter with the ideal emitter was compared, and the potential of cooling power was calculated.

4.1.1. Effect of width (w) of the unit cell on spectral emissivity of the emitter

The impact of width (w) of the unit cell on the spectral emissivity of a selective emitter is shown in Fig. 2(a) and (b). As shown in figure, the emissivity of the designed

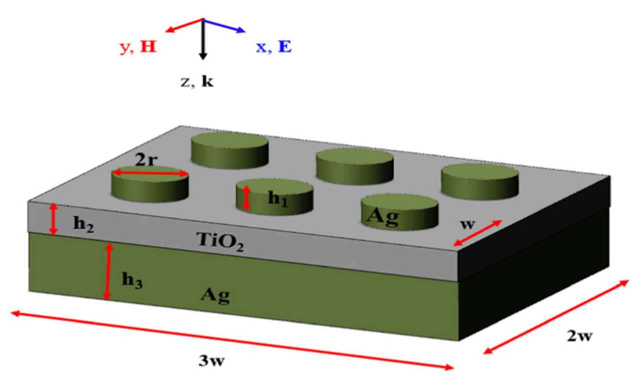

Fig. 1 Schematic representation of the designed MM emitter with disc height (h_1), disc radius (r), dielectric thickness (h_2), ground metal thickness (h_3), and width of unit cell (w)

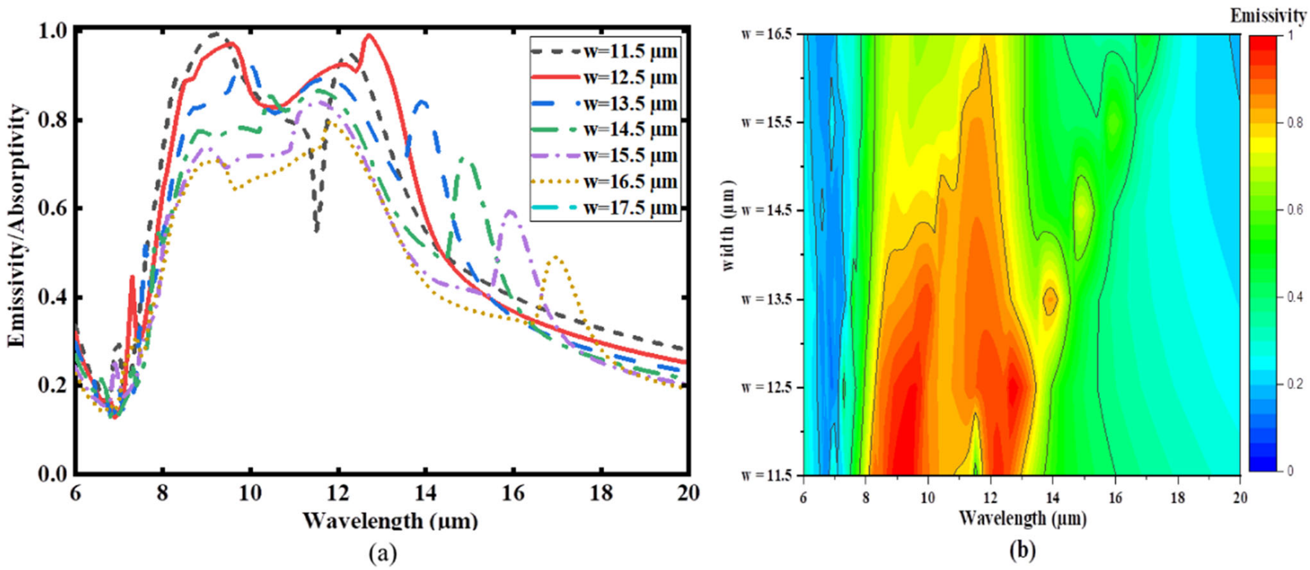

Fig. 2 Effect of width on spectral emissivity of the designed emitter, (**a**) as line graph and (**b**) as colour fill, respectively, when width (w) varies and h_1 = 0.95 μm, h_2 = 1.15 μm, h_3 = 2 μm, and r = 3.6 μm (colour figure online)

emitter was affected by the width of the unit cell. As the width of the unit cell increases from 13.5 to 16.5 μm, the emissivity of the emitter decreases in the required atmospheric transparency window (8–13 μm). This result suggested that the width (w) of the unit cell influences and minimizes the emissivity of the emitter. In general, width (w) of the unit cell has strong effect on the emissivity of the emitter. When the width (w) of the unit cell is 11.5 μm, the emissivity of the designed emitter was high, but it is not broadband in the required atmospheric transparency window.

From the optimized width (w) of the unit cell, we have obtained the widest and most near perfect broadband emissivity of our emitter when the width (w) of the unit cell is 12.5 μm (red colour) in the required atmospheric transparency window (8–13 μm). When the width (w) of the unit cell is 12.5 μm, the emissivity of the emitter has different a peak at in the atmospheric transparency window. These peaks obtained at the wavelength are 9.2 μm and 12.5 μm, and their corresponding emissivity are 96.3% and 97.9%, respectively.

4.1.2. *Effect of dielectric thickness (**h_2**) on the spectral emissivity of the emitter*

As illustrated in Fig. 3(a) and (b), the emissivity of the designed MM emitter depends on the thickness of the dielectric layer. When h_2 increases from 0.65 to 1.65 μm, the emissivity slightly increases. The broadband and high emissions of the emitter were obtained when the thickness (h_2) is 1.15 μm (blue colour) in the required atmospheric transparency window (8–13 μm). As shown in the figure, when h_2 = 1.15 μm there are two major peaks. The peaks correspond to the wavelength of 9.6 μm and 12.7 μm with amplitude 97.1% and 99.2%, respectively. Generally, increasing the thickness of the dielectric increases the emissivity of the MM emitter, but when increased more the emissivity increases out of the atmospheric transparency window (8–13 μm).

4.1.3. *Effect of disc radius (r) on the spectral emissivity of the emitter*

Figure 4(a) and (b) shows that the dependence of emissivity of the MM on the radius of the designed disc. When radius (r) increases from 2.4 to 4 μm, the emissivity also increases and becomes broadband in the required atmospheric transparency window (8–13 μm) up to radius equal to 3.6 μm. But, when the radius (r) greater than 3.6 μm, the emissivity of the emitter emit out of the required wavelength. From the optimized radius (r) of the designed disc, we have obtained the widest and most near perfect broadband emissivity of the MM at the radius (r) is 3.6 μm (Green colour), at this radius (r) the average emissivity of the emitter was 89.5% in the required atmospheric transparency window (8–13 μm). When the radius 3.6 μm, two major peaks were observed which caused by excitation of magnetic polariton in the dielectric between Ag layer. These peaks obtained at the wavelength 9.2 μm and 13 μm with amplitude of 99.4% and 99.2%, respectively.

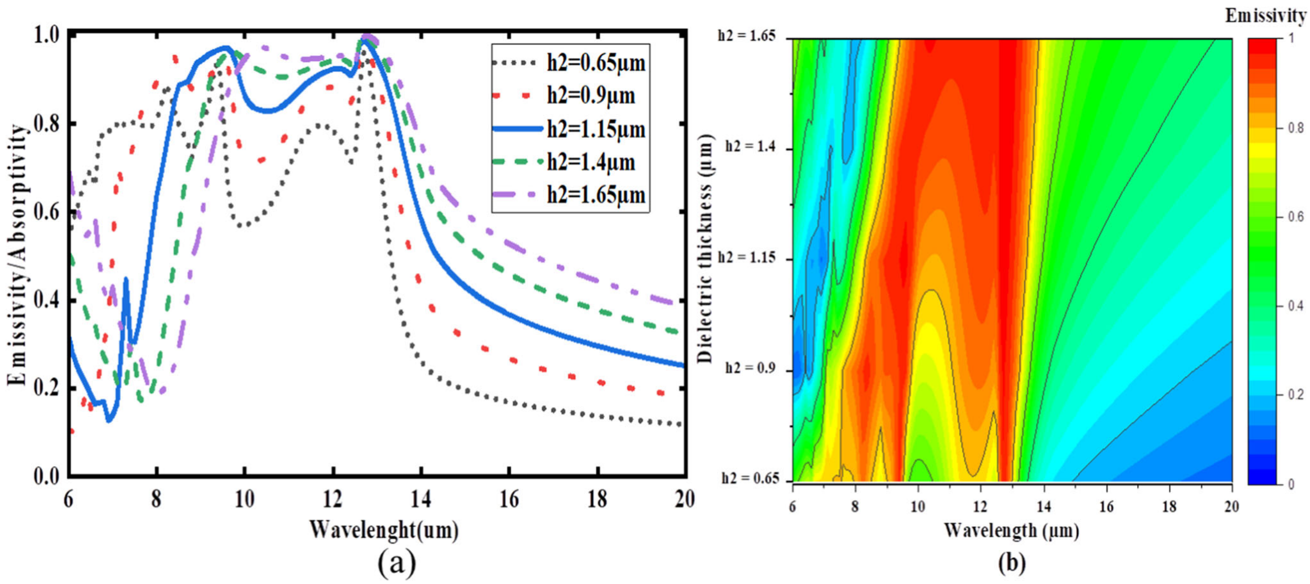

Fig. 3 Effect of dielectric thickness (h_2) on the spectral emissivity of the MM emitter, (**a**) as line graph and (**b**) as colour fills, respectively, when h_2 varies and with other parameters value w = 12.5 μm, h_1 = 0.95 μm, h_3 = 2 μm, and r = 3.6 μm (colour figure online)

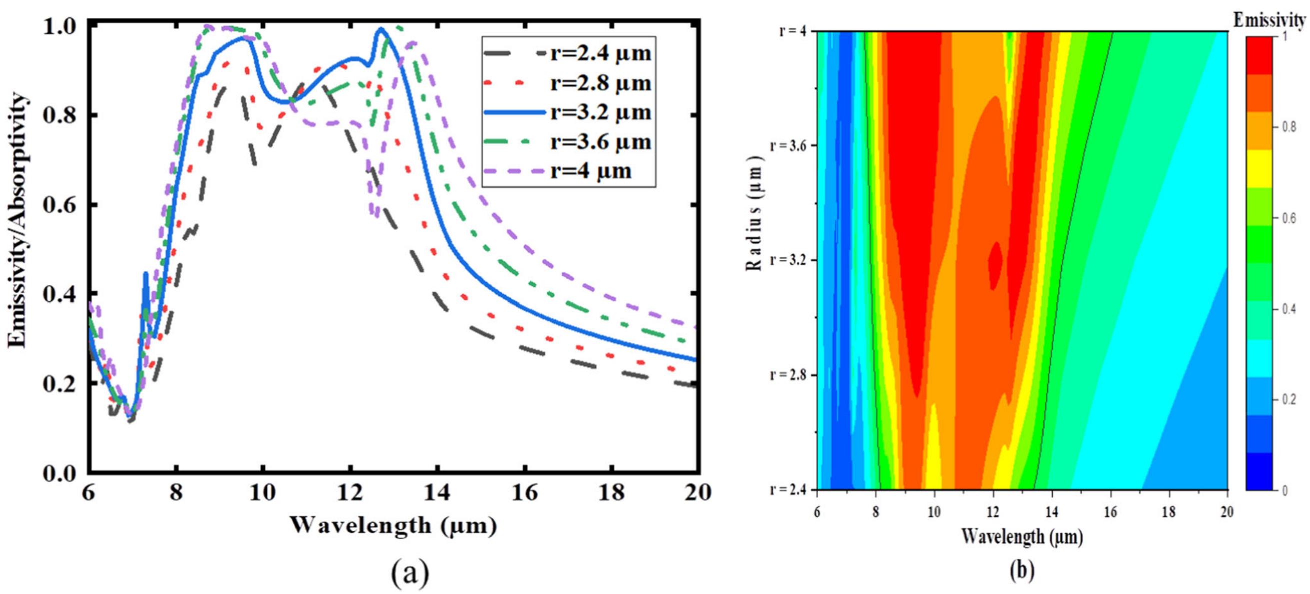

Fig. 4 Effect of disc radius (r) on the spectral emissivity of the MM emitter, (**a**) as lines graph and (**b**) as colour fill, respectively, when radius (r) varies and with other parameters w = 12.5 μm, h_1 = 0.95 μm, h_2 = 1.15 μm, and h_3 = 2 μm (colour figure online)

4.1.4. *Effect of polar angle (θ) on the spectral emissivity of the emitter*

The effect of polarizations and azimuthal angles on spectral emissivity of the designed selective emitter at a normal polar angle ($\theta = 0°$, $\phi = 0°$) was studied. This depicts that the designed emitter is symmetric, which means its polarizations independent. Figure 5(a) and (b) shows the optimized emissivity spectra as the angular emissivity varied from 0 to 60° in 15° steps. Excitation of different physical mechanism was responsible to obtained wide angle spectral emissivity of the designed disc MM. The average emissivity of MM at polar angle $\theta = 0°$ was 89.5% in the atmospheric transparency window (8—13 μm). When the polar angles (θ) increase the emissivity of the emitter gradually increases out of the required atmospheric transparency window (8–13 μm).

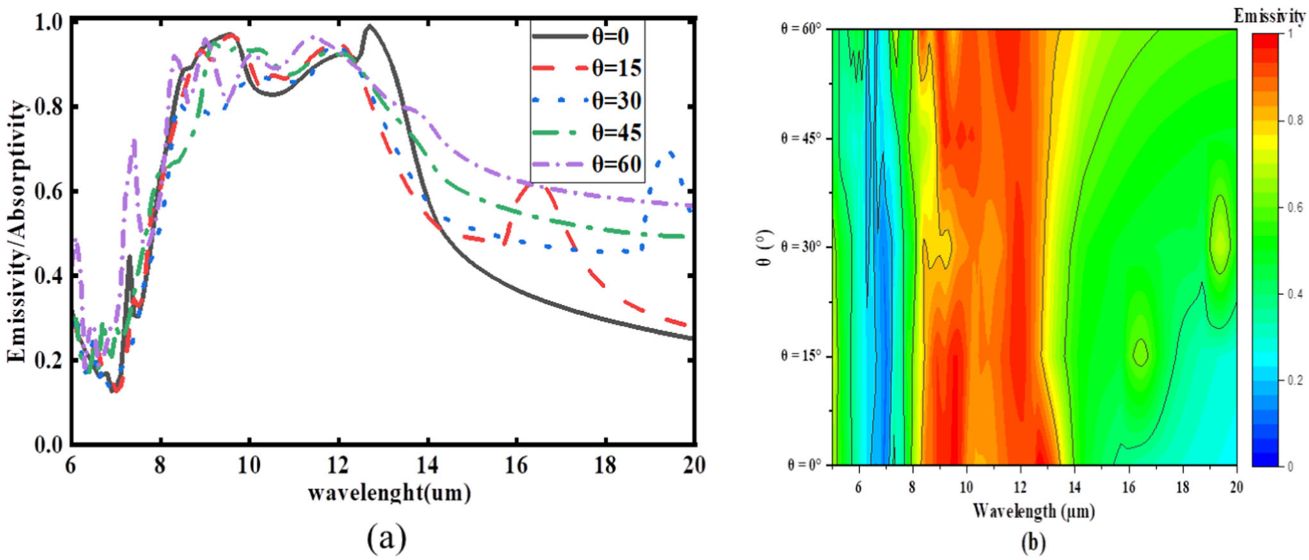

Fig. 5 Emissivity of the designed MM at different angular emissivity, (**a**) as lines graph and (**b**) as colour fill, respectively, and with other parameters of w = 12.5 μm, h_1 = 0.95 μm, h_2 = 1.15 μm, h_3 = 2 μm and r = 3.6 μm (colour figure online)

4.1.5. Effect of dielectric on the spectral emissivity of the emitter

Titanium dioxide (TiO_2) has higher emission than Silicon dioxide (SiO_2) and Aluminium Nitride (AlN) in the mid-infrared or in the second atmospheric transparency window (8–13 μm). The Metal–Dielectric–Metal structure of metamaterial emitter that designed from Silver (Ag) and Titanium dioxide (TiO_2) (i.e. Ag–TiO_2–Ag) has nearly perfect broadband emitter than the MM that designed from Silver (Ag) and Silicon dioxide (SiO_2) (i.e. Ag–SiO_2–Ag) and from Silver (Ag) and Aluminium Nitride (AlN) (i.e. Ag–AlN–Ag) emitter in the required atmospheric transparency window (8 to 13 μm), and which is decreased out of the atmospheric transparency window. The MM with different dielectric such as Titanium dioxide (TiO_2), Silicon dioxide (SiO_2), and Aluminium Nitride (AlN) has an average emissivity of 89.5%, 84.4%, and 86.8%, respectively, in the atmospheric transparency window (8–13 μm). As observed in Fig. 6, the emissivity of our emitter was completely changed when the dielectric is changed. Generally, the emissivity of the designed MM highly affected by dielectric. The effect of this dielectric on the emissivity of the emitter shown in Fig. 6.

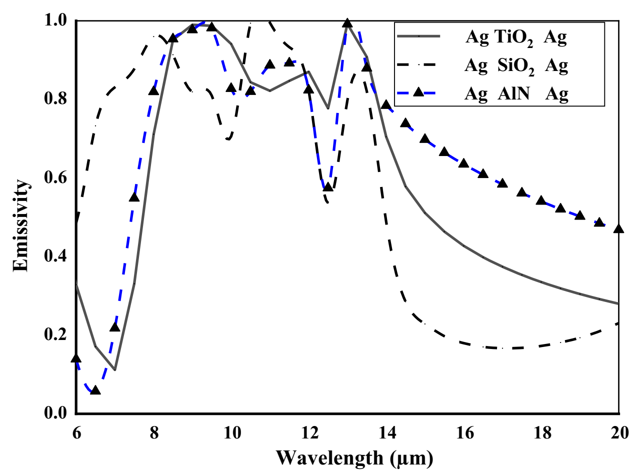

Fig. 6 Effect of dielectric on emissivity spectrum of the designed MM

4.1.6. Performance of the designed MM Emitter

The emissivity of the designed disc MM emitter was high in the atmospheric transparency window. The Metal–Dielectric–Metal (MDM) structure of emitter that designed from Silver (Ag) and Titanium dioxide (TiO_2) (i.e. Ag–TiO_2–Ag) had near perfect broadband emitter in the required atmospheric transparency window (8–13 μm), and which is decreased out of the atmospheric transparency window. But, if the disc is removed from the MM, the emissivity of the designed emitter was strictly decreased. On the other hand, the emissivity of the designed emitter was depend on the structure. By using Metal–Dielectric–Metal structure, we have obtained 89.5% emissivity. This emissivity is the highest value in the atmospheric transparency window. For the flat surface structure, the value of the average emissivity was 21.8% in the atmospheric transparency window (8–13 μm) which is very low emissivity. When our emitter has Metal–Dielectric–Metal structure, the emissivity is high, but when the structure changed from MDM to flat surface the emissivity was completely decreased from 89.5% to 21.8% in the atmospheric transparency window (8–13 μm).

This indicates the performance characteristics of MDM structure of the designed emitter to be high, and our emitter had high cooling power performance. The entire emissivity of MDM structure and flat surface structure of the emitter as comparison of the ideal emitter is shown in Fig. 7.

4.2. Discussion

The radiative cooling power in our calculation investigated over the required atmospheric window from 8 to 13 μm. In order to evaluate the cooling capacity in the emitter, the radiative cooling power in the required transparency window was investigated. It can be clearly observed that the cooling power gets larger with increased ambient temperature. The calculated radiative cooling power is 200.4 W/m^2 at ambient temperature (300 K). By comparing the net cooling power in the relevant work, we have observed that MDM structures are the primary choice to realize effective radiative cooling. But, for inorganic MM thermal emitter, the net cooling power is 194.46 W/m^2 in the first atmospheric transparency window [1]. Again also, for the ultra-broadband all-dielectric MM thermal emitter in [15], the net cooling power in the required atmospheric transparency window is 199 W/m^2, which is lower than that in our design. Therefore, our designed structure achieves an efficient cooling effect.

The designed emitter had high emissivity, because of that high radiative cooling power were obtained in the required atmospheric transparency window. This high emissivity and high radiative cooling power were obtained at the different optimized parameters of the designed MM. From the optimized parameters of the emitter high emissivity and high radiative cooling power were obtained when the width (w) of the unit cell, the thickness (h_2) of the dielectric, and the radius (r) of the disc had the value of 12.5 μm, 1.15 μm, and 3.6 μm, respectively, and by fixed parameters height (h_1) of the disc and the thickness (h_3) of the ground metal had the value of 0.95 μm and 2 μm, respectively. The cooling performance of the MM was compared with the cooling performance of the ideal emitter. Graphically, the comparison of net radiative cooling power between our MM and ideal emitter is shown in Fig. 8.

One way to enhance passive cooling by radiative cooling is to instal thermal emitters on surfaces that radiate heat in atmospheric transparency window. When designing thermal emitters, by taking into account infrared energy transmitted from the atmosphere. Thermal emitters should be designed to emit thermal radiation selectively in the 8–13 μm bands. This band is the atmospheric transparency window. Emitters in this band have enhanced cooling performance as they can reflect incident atmospheric radiation from the non-transparent band. An effectively designed thermal emitter can maintain surface temperatures below the ambient air temperature. The infrared emissivity of the radiative cooling surface must be controlled for each wavelength band. To achieve spectral selective emissivity, researchers have developed photonic crystals [16, 17], electrochromic devices [18], and plasmonic MM. In this research, we developed a Metal–Dielectric–Metal (MDM) structure for radiative cooling application. This emitter exhibits improved radiative cooling performance.

The global AM1.5 solar spectrum has an irradiance of 1000 W/m^2 and considers solar reflectors integrated on the top of emitters, so (ignore P_{sun}). By insulating back surface of the emitter with plastic foam (polystyrene) the

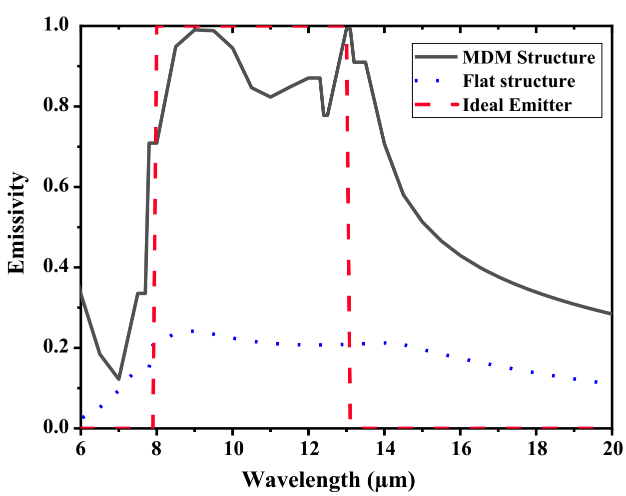

Fig. 7 Entire emissivity spectrums of our MDM structure and Flat structure emitter as comparison with the ideal emitter as a function of wavelength

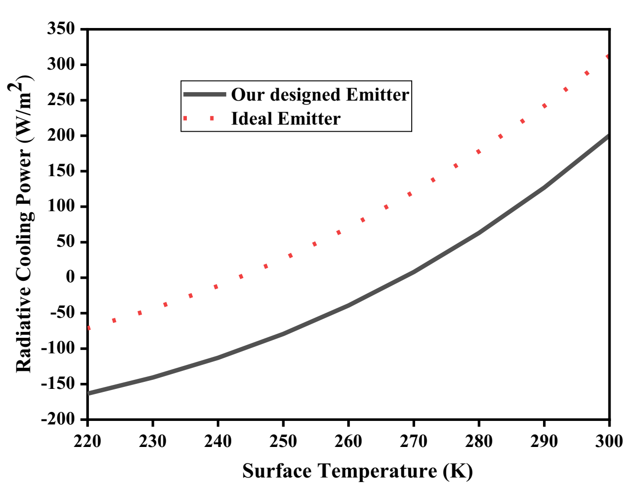

Fig. 8 Comparison of net cooling power between our MM emitter and the ideal emitter ($T_{amb} = 300$ K)

conductive heat coefficient from the back surface to the air can be minimized or (ignore $P_{cond+conv}$). We excluded conduction and convection induced by solar irradiation from our analysis. Solar irradiation is concentrated in the visible range. Surface radiation and atmospheric radiation mainly occurs in the infrared band. Therefore, the absorbed power from solar irradiation is possible to the radiative cooling performance only considered surface and atmosphere radiation to evaluate total radiative cooling performance. In addition, the absorption of solar irradiation is very sensitive to environmental conditions such as the time, latitude, weather, and season. The temperature gradient between a surface and the atmosphere is reduced by both convective and conductive heat transfer. It is difficult to evaluate the heat transfer coefficient quantitatively as it is affected by the surface and atmosphere temperatures in addition to the environmental conditions. We did not consider conduction and convection arising from solar irradiation as a result of these considerations. Instead, we analysed the radiative cooling performance of solid surfaces with respect to atmospheric and surface radiation.

The infrared transparency window of the atmosphere is between 8 and 13 μm. Passive cooling is possible in this band because surfaces that emit radiation in this window absorb low levels of atmospheric radiation. Atmospheric radiation from the non-transparent regions irradiates solid surfaces. This absorption is characterized by the absorptivity of the surface. Broadband radiation emitters have limited cooling performance as they absorb a lot of atmospheric radiation. As we can control the radiation characteristics of MDM structures, we developed an MDM-based spectral selective emitter and we measured the spectral emissivity of the designed structure in the direction of the zenith and at an incline. We also simulated structures of different sizes to determine the effect of varying the size of the structure on the emissivity.

We optimized different parameters such as width of the unit cell, thickness of the dielectric, and radius of disc. Those parameters highly affect the emissivity of the designed emitter, whereas the fixed parameters such as the height of disc and the thickness of the ground metal do not affect the emissivity of the emitter.

Passive cooling and night-time cooling are areas of focus due to several reasons such as energy efficiency, environmental sustainability, cost-effectiveness, resilience to power outages, utilizing night-time cooling potential, and offsetting climate change and urban heat islands. These reasons highlight the importance of focusing on passive cooling and night-time cooling as effective and sustainable approaches for reducing energy consumption, decreasing environmental impact, improving resilience, and enhancing comfort in various settings.

5. Conclusions

In this work, we proposed and numerically analysed metal–dielectric–metal structure of MM selective emitter for radiative cooling applications. Radiative coolers are optically designed to reject heat to outer space through the atmospheric window spectral band (8–13 μm). Radiative cooling performance can be improved by using a spectral selective emitter that is designed to reflect atmospheric radiation and unilaterally radiate through the infrared atmosphere transparency window. As the surface emissivity increases, the cooling performance improves until the temperatures of the surface and the atmosphere become same ($T_s - T_{amb} = 0$).

The potential application of this MM emitter can be used for radiative cooling application. A simplified structure which produces a good radiative cooling power was also obtained. We have shown that it is possible to design structures, which are very emissive in the atmospheric transparency window. The disc structures illustrate the unique ability for a strictly selective and robust thermal emissivity within the required atmospheric transparency window. Our approach shows that instead of using bulk materials, especially designed MDM structures can be engineered to yield superior characteristics for engineered thermal radiation. Utilizing its broadband emission spanning over the entire 8–13 μm atmospheric transparency window of the atmosphere, the disc emitters can appear as emerging candidate for liberating heat directly to the free outer space.

In summary, we have designed and theoretically demonstrated a thermal emitter for high-performance radiative cooling, based on disc structure consisting of Ag and TiO_2. Through utilizing the electromagnetic resonance modes and anti-reflection of the MM, near-ideal unity emissivity in the required atmospheric windows is achieved, which provides a radiative cooling power over 200.4 W/m^2 at the ambient temperature (300 K), and there is a potential to reach an equilibrium temperature of 268.25 K. Even the emitter holds the potential of cooling down 31.75 °C below the ambient temperature.

Author contributions All authors contributed to the study's conception and design. The processes of conceptualizing, designing, data analysis, and interpretation were performed by all authors (WM and FT). The first draft of the manuscript was written by WM, and all authors commented on previous versions of the manuscript. All authors read and approved the final manuscript after critical revision. All authors met the requirements for authorship, and they confirm that the manuscript represents honest work.

Declarations

Conflict of interest The authors declare that they have no known competing financial interests or personal relationships that could have appeared to influence the work reported in this paper.

References

[1] H Yin, H Yao, Y Jia, J Wang and C Fan *J. Phys. D: Appl. Phys.* **54** 345501 (2021)
[2] V Chetan, K Nagaraj, P S Kulkarni, S K Modi and U N Kempaiah *J. Phys.: Conf. Ser.* **1473** 012054 (2020)
[3] X Liu, T Tyler, T Starr, A F Starr, N M Jokerst and W J Padilla *Phys. Rev. Lett.* **107** 045901 (2011)
[4] X Sun, Y Sun, Z Zhou, M A Alam and P Bermel *Nanophotonics* **6** 997 (2017)
[5] M Li, H B Peterson and C F Coimbra *J. Renew. Sustain. Energy* **11** (2019)
[6] X Lu, P Xu, H Wang, T Yang and J Hou *Renew. Sust. Energ. Rev.* **65** 4800 (2016)
[7] R Family and M P Mengüç *Sustainability* **10** 3049 (2018).
[8] Y Li, L Li, L Guo and B An *Opt. Mater. Express* **10** 1767 (2020)
[9] B Ko, D Lee, T Badloe and J Rho *Energies* **12** 89 (2019)
[10] Y Dai, Z Zhang and C Ma *Opt. Commun.* **475** 126231 (2020)
[11] D Chae, M Kim, P H Jung, S Son, J Seo, Y Liu, J L Bong and H Lee *ACS Appl. Mater. Interfaces* **12** 8073 (2020)
[12] Suhendri, M Hu, Y Su, J Darkwa and S Riffat *Buildings* **10** 215 (2020)
[13] Y Zhu, Y H Ye, D Wang and Y Cao *AIP Adv.* **11** (2021)
[14] M A Kecebas, M P Menguc, A Kosar and K Sendur *J. Quant. Spectrosc. Radiat. Transf.* **198** 1339 (2017)
[15] A Kong, B Cai, P Shi and X C Yuan *Opt. Express 27* 30102 (2019)
[16] W Zhang, G Xu, J Zhang, H Wang and H Hou *Opt. Mater.* **37** 343 (2014)
[17] W Zhang, G Xu, J Zhang, H Wang and H Hou *Appl. Phys. Lett.* **81** 4685 (2003)
[18] A Bessière, C Marcel, M J Morcrette, M Tarascon, V Lucas, B Viana and N J Baffier *Appl. Phys.* **91** 1589 (2002)